

# Munc18a controls SNARE assembly through its interaction with the syntaxin N-peptide

Pawel Burkhardt<sup>1</sup>, Douglas A Hattendorf<sup>2,3</sup>, William I Weis<sup>2,3</sup> and Dirk Fasshauer<sup>1,\*</sup>

<sup>1</sup>Research Group Structural Biochemistry, Department of Neurobiology, Max-Planck-Institute for Biophysical Chemistry, Göttingen, Germany, <sup>2</sup>Department of Structural Biology, Stanford University School of Medicine, Stanford, CA, USA and <sup>3</sup>Department of Molecular and Cellular Physiology, Stanford University School of Medicine, Stanford, CA, USA

**Sec1/Munc18-like (SM) proteins functionally interact with SNARE proteins in vesicular fusion. Despite their high sequence conservation, structurally disparate binding modes for SM proteins with syntaxins have been observed. Several SM proteins appear to bind only to a short peptide present at the N terminus of syntaxin, designated the N-peptide, while Munc18a binds to a 'closed' conformation formed by the remaining portion of syntaxin 1a. Here, we show that the syntaxin 16 N-peptide binds to the SM protein Vps45, but the remainder of syntaxin 16 strongly enhances the affinity of the interaction. Likewise, the N-peptide of syntaxin 1a serves as a second binding site in the Munc18a/syntaxin 1a complex. When the syntaxin 1a N-peptide is bound to Munc18a, SNARE complex formation is blocked. Removal of the N-peptide enables binding of syntaxin 1a to its partner SNARE SNAP-25, while still bound to Munc18a. This suggests that Munc18a controls the accessibility of syntaxin 1a to its partners, a role that might be common to all SM proteins.**

*The EMBO Journal* (2008) 27, 923–933. doi:10.1038/emboj.2008.37; Published online 13 March 2008

**Subject Categories:** membranes & transport

**Keywords:** membrane fusion; Munc18; neurosecretion; SNARE; syntaxin

## Introduction

Transport of cargo between organelles in eukaryotic cells is mediated by vesicles that bud from a donor compartment and specifically fuse with an acceptor membrane. The central machinery involved in the fusion process is composed of members of the SNARE (soluble N-ethylmaleimide-sensitive factor attachment receptor) protein family. SNAREs anchored in the vesicle and target membrane are thought to assemble in a zipper-like fashion into a four-helix bundle, providing the energy to drive fusion of the two bilayers (Hong, 2005; Jahn and Scheller, 2006). Although SNAREs are sufficient to drive membrane fusion when inserted into liposome membranes (Weber *et al*, 1998; Pobbati *et al*, 2006), this minimal

machinery is organized and controlled by additional factors *in vivo*.

Members of the cytosolic Sec1/Munc18-like (SM) family of proteins have been established as essential factors in different intracellular transport steps, during which they functionally interact with the SNARE machinery. However, the molecular basis for this interaction is not entirely understood. In particular, the SM protein Munc18a (also known as Unc18, nSec1, and Rop) has an ambiguous role in the Ca<sup>2+</sup>-dependent discharge of neurotransmitter from synaptic vesicles (reviewed by Rizo and Sudhof, 2002; Gallwitz and Jahn, 2003; Toonen and Verhage, 2003, 2007; Weimer and Richmond, 2005; Burgoyne and Morgan, 2007). This vesicular fusion step is mediated by a well-characterized set of SNAREs, consisting of the synaptic vesicle protein synaptobrevin/VAMP 2 and the two plasma membrane proteins syntaxin 1a and SNAP-25. Munc18a binds with nanomolar affinity to syntaxin 1a (Pevsner *et al*, 1994). The cytosolic domain of syntaxin 1a contains a conserved N-terminal peptide, followed by a three-helix bundle designated Habc (Fernandez *et al*, 1998), a linker, and the H3 domain, which forms one of the helices in the SNARE complex. When bound to Munc18a, syntaxin 1a adopts a 'closed' conformation in which the H3 domain folds back onto Habc, rendering it inaccessible to its partner SNAREs (Pevsner *et al*, 1994; Dulubova *et al*, 1999; Misura *et al*, 2000; Yang *et al*, 2000). Therefore, for syntaxin 1a, to assemble into a SNARE complex, it is thought that it must dissociate from Munc18a and switch to an open conformation in which the H3 domain is accessible. Dissociation of the Munc18a–syntaxin 1 complex, however, is a slow process (Pevsner *et al*, 1994), which is likely related to the extensive interaction surface between syntaxin 1a and the clamp-like structure formed by the three domains of Munc18a (Misura *et al*, 2000).

Although biochemical and structural data imply an inhibitory role for Munc18, loss of Munc18a function blocks neurotransmitter release, indicating that this molecule has an essential, positive role in neuronal secretion (Weimer and Richmond, 2005). Studies of other SM proteins that serve in different intracellular trafficking pathways also support an activating role for this family (Toonen and Verhage, 2003; Weimer and Richmond, 2005). A binding mode distinct from that of Munc18a–syntaxin 1a appears to govern the interaction of several SM proteins with their cognate syntaxins, in particular, between Sly1 and Sed5/syntaxin 5, and Vps45 and Tlg2/syntaxin 16. In these complexes, the very N-terminal region of the syntaxin preceding the Habc domain, designated the N-peptide, binds to the outer surface of the SM domain 1 (Bracher and Weissenhorn, 2002; Dulubova *et al*, 2002; Peng and Gallwitz, 2002), opposite the domain 1 surface that interacts with the closed conformation of syntaxin 1a. Unlike Munc18a, these other SM proteins are thought not to interact with the remainder of their cognate syntaxin molecule, suggesting that the N-peptide interaction somehow assists in the formation of SNARE complexes rather than

\*Corresponding author. Department of Neurobiology, Max-Planck-Institute for Biophysical Chemistry, Göttingen, Am Fassberg 11, 37077 Germany. Tel.: +49 551 201 1637; Fax: +49 551 202 1499; E-mail: dfassha@gwdg.de

Received: 27 November 2007; accepted: 12 February 2008; published online: 13 March 2008

inhibiting access of the syntaxin SNARE motif (Rizo and Sudhof, 2002; Gallwitz and Jahn, 2003; Toonen and Verhage, 2003, 2007; Weimer and Richmond, 2005; Burgoyne and Morgan, 2007). As Munc18a does not bind detectably to the isolated N-peptide of syntaxin 1a (Dulubova *et al*, 2003; Shen *et al*, 2007), it was thought that it cannot mediate a comparable role in vesicle fusion. A third mode of SM function appears to occur in yeast Sec1p, which does not bind to the plasma membrane syntaxin Sso1p, but can instead bind to the assembled plasma membrane SNARE complex (Scott *et al*, 2004; Togneri *et al*, 2006).

Recent findings have begun to address the apparent discrepancies in the mechanisms of SM proteins. The isolated N-peptide of syntaxin 4 is able to bind to the outer surface of Munc18c, in a manner similar to that observed in the Sly1–Sed5 complex (Hu *et al*, 2007). Munc18c and syntaxin 4 are closely related to Munc18a and syntaxin 1a. Furthermore, Munc18a can bind to an assembled SNARE complex (Dulubova *et al*, 2007; Khvotchev *et al*, 2007; Shen *et al*, 2007), and this interaction requires the syntaxin N-peptide. As the N-peptide alone is not sufficient for binding, it is clear that other regions of the SNAREs must participate in the interaction.

Based on these data, it has been proposed that when bound to the assembled SNARE complex via the syntaxin N-peptide, Munc18a somehow stimulates the membrane fusion reaction. This configuration is believed to be similar to the binding mode employed by Sly1/Sed5 (endoplasmic reticulum-Golgi trafficking), Vps45/syntaxin 16 (endosomal trafficking), and Munc18c/syntaxin 4 (regulated secretion in a variety of cell types), thus providing a common interaction mechanism between SM proteins and syntaxins. In contrast, the tight interaction between Munc18a and the closed conformation of syntaxin 1a was proposed to represent an

additional role of Munc18a, either in sequestering syntaxin 1a from other SNAREs (Shen *et al*, 2007) or in the process of docking and priming of the vesicle (Dulubova *et al*, 2007). This latter binding mode was suggested to be specific for SM proteins of the Munc18a-like type involved in regulated secretion.

Although these models appear to explain some of the SM properties, they do not answer a critical question regarding the neuronal system: how can syntaxin 1a escape the tight grip of Munc18a to participate in SNARE complex formation? Moreover, the models are based on semiquantitative protein-binding assays, and the effect of Munc18a on the kinetics of SNARE assembly has not been examined. Here, we provide thermodynamic, kinetic, and structural data indicating that the conserved N-peptide of syntaxin 1a acts as a switch controlling the binding of Munc18a to the closed, inhibited conformation of syntaxin 1a or to the SNARE complex. We also find that Vps45 interacts detectably with the N-peptide of syntaxin 16, but the interaction is stronger when the remainder of syntaxin 16 is present. These findings suggest that both modes of interaction may occur in many SM–syntaxin pairs.

## Results

### **The syntaxin 1a N-peptide contributes to the affinity for Munc18a**

Isothermal titration calorimetry (ITC) and fluorescence spectroscopy were used to accurately measure the thermodynamics and kinetics of the Munc18a–syntaxin 1a interaction. The cytosolic domain of syntaxin 1, Syx1a (1–262), binds to Munc18 with a favourable binding enthalpy ( $\Delta H \approx -35$  kcal/mol) and a dissociation constant  $K_d$  of approximately 1 nM (Table I; Figure 1), which is at the lower limit of the ITC instrument. This high affinity was confirmed by

**Table I** Thermodynamic parameters of the interaction of syntaxins and SM proteins measured by ITC

Interaction of	$K_d$ (nM)	$\Delta H^\circ$ (kcal/mole)	$n$
Syx1a (1–262)/Munc18a	1.4 ± 0.3	−34.6 ± 0.2	1.03
Syx1a (1–240)/Munc18a	2.7 ± 0.6	−34.3 ± 0.4	1.01
Syx1a (1–226)/Munc18a	621.1 ± 107.2	−8.0 ± 0.5	0.84
Syx1a (1–179)/Munc18a	693.9 ± 84.2	−5.5 ± 0.5	0.91
Syx1a (1–20)/Munc18a	—	—	—
Syx1a (25–262)/Munc18a	8.1 ± 1.0	−25.1 ± 0.2	1.01
Syx1a (180–262)/Munc18a	—	—	—
Syx1a (180–262) + Syx1a (1–179)/Munc18a	277.8 ± 33.7	−21.2 ± 0.8	0.94
Syx1a <sup>LE</sup> /Munc18a	7.7 ± 0.6	−34.8 ± 0.2	0.99
Syx1a <sup>I235A</sup> /Munc18a	333.3 ± 58.4	−16.0 ± 0.7	0.93
Syx1a <sup>R4A</sup> /Munc18a	9.4 ± 1.6	−27.3 ± 0.3	1.03
Syx1a <sup>T5A</sup> /Munc18a	1.9 ± 0.7	−32.6 ± 0.3	1.01
Syx1a <sup>L8A</sup> /Munc18a	9.1 ± 1.7	−27.3 ± 0.3	1.01
Syx1a <sup>T10A</sup> /Munc18a	0.4 ± 0.2	−34.6 ± 0.2	1.05
Syx1a <sup>S14A</sup> /Munc18a	2.6 ± 1.3	−33.5 ± 0.4	1.03
SNARE complex containing Syx1a (1–262)/Munc18a	719.4 ± 118.0	−4.8 ± 0.4	0.84
SNARE complex containing Syx1a (25–262)/Munc18a	—	—	—
Syx16 (1–302)/Vps45	2.1 ± 1.2	−23.8 ± 0.2	1.09
Syx16 (1–279)/Vps45	0.85 ± 0.3	−26.3 ± 0.1	0.96
Syx16 (1–265)/Vps45	11.7 ± 3.6	−13.6 ± 0.2	1.07
Syx16 (1–183)/Vps45	32.5 ± 0.3	−12.0 ± 0.1	0.93
Syx16 (1–27)/Vps45	26.9 ± 0.3	−11.6 ± 0.1	0.95
Syx16 (1–27) <sup>F10A</sup> /Vps45	—	—	—
Syx16 (1–302) <sup>F10A</sup> /Vps45	116.6 ± 16.5	−15.6 ± 0.5	0.85
Syx16 (28–302)/Vps45	—	—	—

All isothermal calorimetric experiments were performed at 25°C in PBS buffer. The experimental ITC data for the interaction of Munc18a and syntaxin 1a variants and for Vps45 and syntaxin 16 variants are shown, respectively, in Supplementary Figures 6 and 7.

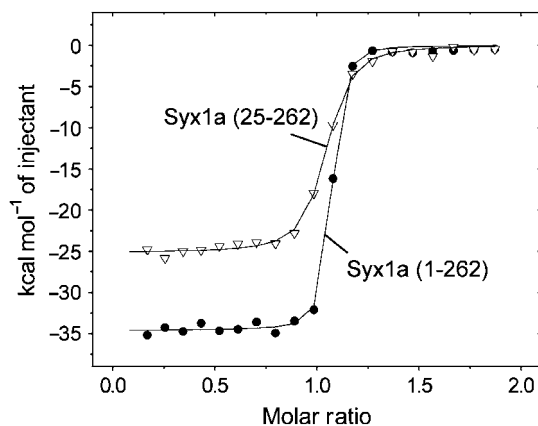


**Figure 1** The N-peptide participates in binding of syntaxin 1a to Munc18a. Calorimetric titrations of Syx1a (1–262 or 25–262) into Munc18a. Shown are the integrated areas normalized to the amount of syntaxin 1a (kcal/mol) versus the molar ratio of syntaxin to Munc18a. The solid lines represent the best fit to the data for a single binding site model using a nonlinear least squares fit.

using the increase in tryptophan fluorescence upon binding and also by determining the dissociation and association rate constants, which gave a  $K_d$  of 0.3 nM (Supplementary Figure 1). Our findings are in agreement with the affinity of 5.7 nM determined by surface plasmon resonance spectroscopy experiments in which soluble Munc18 was flowed over immobilized syntaxin 1a (Pevsner *et al*, 1994). The surface plasmon resonance experiments also gave an association rate constant of  $k_{on} \approx 42000 \text{ M}^{-1} \text{ s}^{-1}$  and a dissociation rate constant of  $k_{off} \approx 0.00024 \text{ s}^{-1}$ . When we measured the rate of dissociation in solution, we observed a roughly 10-fold increase in the dissociation rate constant ( $k_{off} \approx 0.0011 \text{ s}^{-1}$ ) and a 100-fold increase the association rate constant ( $\approx 5 \times 10^6 \text{ M}^{-1} \text{ s}^{-1}$ ) (Supplementary Figure 1).

Remarkably, a syntaxin 1a variant, Syx1a (25–262), in which the 24 N-terminal residues are removed showed a reduced affinity ( $K_d \approx 8 \text{ nM}$ ), accompanied by a clear decrease in binding enthalpy ( $\Delta H^\circ \approx -25 \text{ kcal/mol}$ , Figure 1). The difference in binding enthalpy very likely reflects the additional contribution of the syntaxin 1a N-peptide to the interaction.

### **The syntaxin 1a N-peptide is seen in the structure of the Munc18a–syntaxin 1a complex**

The finding that the N-peptide of syntaxin 1a enhances the affinity of the Munc18a/syntaxin1a interaction led us to re-examine the published structure of the Munc18a/Syx1a complex. We originally reported that the first 26 residues of syntaxin1a could not be modelled into the electron density and were therefore likely to be disordered (Misura *et al*, 2000). However, there was some significant, but uninterpretable, residual electron density on the outer surface of domain 1 of Munc18a, which the subsequent structures of Munc18c–syntaxin4 (Hu *et al*, 2007) and Sly1–Sed5 (Bracher and Weissenhorn, 2002) revealed as the N-peptide-binding site. Using these other structures as a guide, we could place the conserved Asp3–Arg4–Thr5 (DRT) motif of the syntaxin1a peptide into this density. Re-refinement of the published structure (Table II) improved the electron density in this region, and residues 2–9 of syntaxin 1a could be modelled

(Figure 2A). Thus, the N-peptide of syntaxin1a binds to its predicted site (Hu *et al*, 2007) on Munc18a, while the Habc and SNARE domain are bound in the closed conformation to a second site on the inside of the Munc18a arch (Figure 2B).

The overall structure of the bound syntaxin 1a N-peptide is similar to that of syntaxin 4 bound to Munc18c (Figure 3). In both cases, a short extended structure at the N terminus is followed by a short  $\alpha$  helix. As described previously (Hu *et al*, 2007), the conserved DRT motif appears to stabilize the observed conformation through intramolecular side chain hydrogen bonds between Asp3 and Thr5, and Arg4 and Glu7. However, syntaxin 1a forms only 4 hydrogen bonds and  $\sim 40$  van der Waals contacts with Munc18a, whereas syntaxin 4 forms 13 hydrogen bonds and  $\sim 140$  van der Waals contacts with Munc18c (Figure 3). This is due, in part, to sequence differences in the peptide-binding site. For example, Asp3 of syntaxin 4 interacts with the side chains of Arg132 and Lys134 of Munc18c; these residues are replaced by threonine in Munc18a, and are not positioned to contact the Asp3 side chain. Also, Glu223 in the  $\alpha 8$  loop in domain 2 of Munc18c forms a hydrogen bond with the main-chain nitrogen of Asp3; in Munc18a, the  $\alpha 8$  loop is in a different conformation.

Although sequence differences can explain some of the smaller number of interactions observed between the syntaxin 1a N-peptide and Munc18a relative to syntaxin 4–Munc18c, contacts involving certain conserved residues are also lost or diminished. Most notably, syntaxin 1a Leu8 is not well packed into the hydrophobic pocket formed by residues Phe115, Val119, Ala124, Ile127, and Leu130 of Munc18a. Electron density for the side chain of Leu8 is weak, suggesting that it may be present in multiple conformations. In addition, syntaxin 1a Arg4 is too far from the carbonyl oxygen of Munc18a Cys110 to form the hydrogen bond seen in the syntaxin 4–Munc18c structure.

Given the observed differences in the interactions of conserved residues in the syntaxin1a–Munc18a versus syntaxin4–Munc18c, we investigated the contribution of conserved syntaxin 1a N-peptide residues to the affinity of the Munc18a interaction by ITC (Table I). Thr10 is not seen in the structure, and its mutation does not affect binding. On the other hand, mutation of Ser14, which is not seen in the structure, slightly diminishes the interaction. Most notably, mutation of Arg4 or Leu8 to alanine reduces the affinity and enthalpy of the reaction to the same values as complete removal of the peptide, indicating that despite the fewer number of contacts made by these residues, they have essential roles in the Munc18a interaction. These results suggest that the conformation of the syntaxin1A N-peptide in the crystal has been perturbed relative to its Munc18a-bound conformation in solution. Crystal packing interactions between neighbouring syntaxin 1a N-peptides (Figure 2B) could influence the conformation of the peptide, although there is no obvious explanation for why the observed lattice contacts would prevent formation of the predicted syntaxin1a–Munc18a contacts. The more likely reason for the loss of expected contacts comes from the fact that the syntaxin construct used for crystallization bears an N-terminal polyhistidine affinity tag. This construct binds to Munc18a with an affinity intermediate between full-length syntaxin bearing no extra residues at its N terminus and the truncated syntaxin Syx1a (25–262) (see Supplementary data; Supplementary Figure 2), suggesting

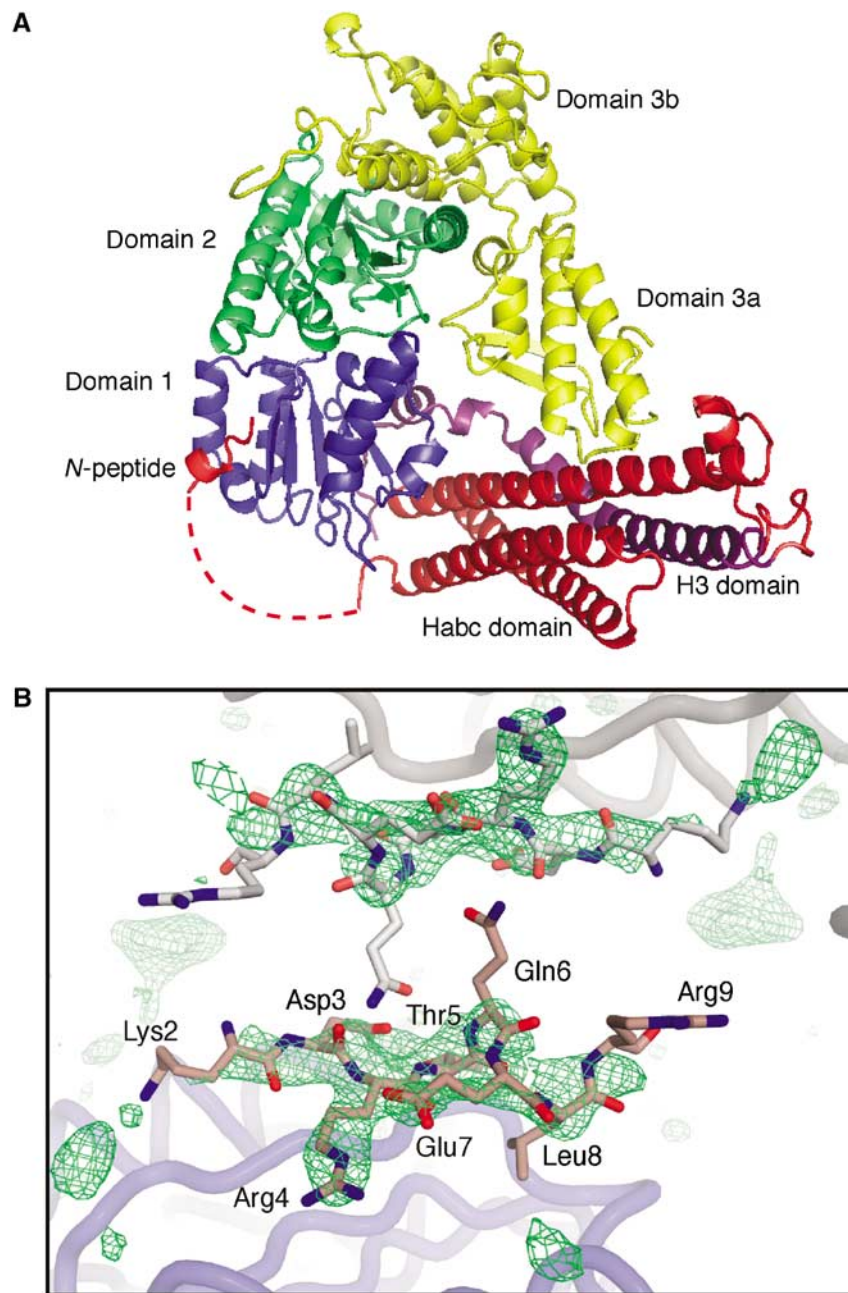


**Figure 2** Newly refined crystal structure of the Munc18a-syntaxin1a complex. (A) Munc18a domains 1, 2, and 3 are defined as described (Misura *et al*, 2000) and coloured blue, green, and yellow, respectively. The H3 SNARE domain of syntaxin is coloured purple, and the regulatory Habc domain and N-terminal peptide are coloured red. The dashed line represents residues 10–26 of syntaxin, which are not visible in the electron density maps. (B)  $F_o - F_c$  omit map. Positive electron density is shown in green at a  $3.0\sigma$  contour. The syntaxin N-terminal peptide is shown in stick representation in dark salmon, and a symmetry-related peptide in the crystal is shown in light grey. The map was calculated by omitting the peptide during final round of refinement.

that the tag partially interferes with peptide binding. In this regard, it should also be noted that we found that thrombin, a protease that is widely used to specifically cleave affinity tags of recombinant proteins, removes the first nine residues of syntaxin 1a, rendering the N-peptide unable to bind to Munc18a. A detailed account of the effect of affinity tags on the syntaxin–Munc18 interaction is provided in the Supplementary data.

The effect of the N-terminal affinity tag indicates that a detailed description of the syntaxin 1a N-peptide interaction with Munc18a will require crystallization of a construct with

a native N terminus. Nonetheless, the crystallographic data clearly demonstrate that the syntaxin N-peptide interacts with the outer surface of Munc18a domain 1 in a manner similar to other syntaxin–Munc18 pairs, and are consistent with the increases in binding affinity and enthalpy observed in the ITC experiments.

#### **Contribution of the three regions of syntaxin 1a to Munc18a interactions**

The results presented so far indicate that all conserved regions of syntaxin 1a interact with Munc18a: the N-peptide

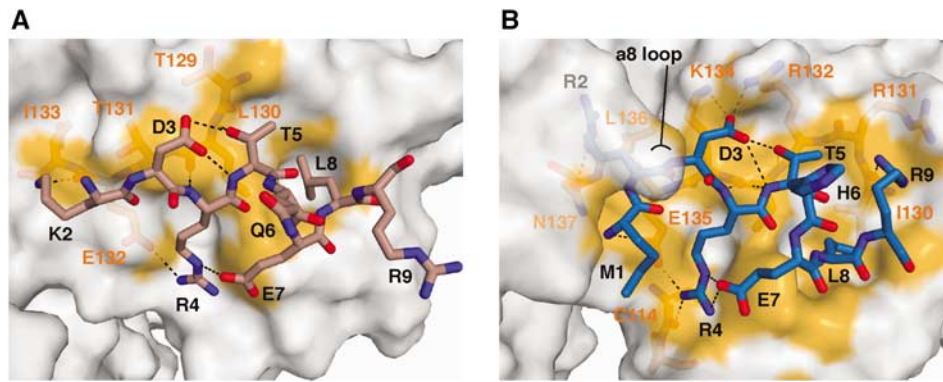


**Figure 3** Comparison of syntaxin N-terminal peptide-binding sites on (A) Munc18a and (B) Munc18c. In each case, the Munc18 homologue is shown in surface representation, with the surface formed by atoms that contact syntaxin coloured orange. Residues that form hydrogen bonds with syntaxin are shown beneath the surface, with the hydrogen bonds shown as dashed lines. In (A), the syntaxin 1A peptide is coloured dark salmon. In (B), the syntaxin 4 is light blue. Residues 10–19, which were only observed in the Munc18c-syntaxin4 structure, are not shown. Note that in (B), Glu233, which is located in the  $\alpha 8$  loop and interacts with Asp3, is not shown for clarity.

binds to the outer surface of Munc18a domain 1, while the Habc, linker, and H3 regions interact with the concave surface formed by domains 1 and 3a (Misura *et al*, 2000). Approximately equal numbers of residues from the Habc and H3 domains contribute to the syntaxin 1a–Munc18a interaction. Habc forms an independently folded domain whose structure is essentially unaltered whether free or bound to Munc18a. In contrast, the structure of H3 depends on context, where it is a single helix in the SNARE complex, but three helices interrupted by irregular sections when it is bound to the Habc domain in the closed conformation (Misura *et al*, 2000).

To dissect the energetic contributions of the different portions of the syntaxin cytosolic domain to the Munc18a interaction, the thermodynamics of N- and C-terminal deletion constructs were measured by ITC (Table I). As noted above, removal of the N-peptide reduces the affinity from  $\sim 1$  to 8 nM ( $\Delta\Delta G^\circ = 1.2$  kcal/mol). If we assume that this peptide binds independently of the remainder of syntaxin, this energy corresponds to a  $K_d$  of 130 mM, explaining why no detectable binding of the peptide is observed to either Munc18a or Munc18a–Syx1a (25–262). In contrast, removal of C-terminal sequences has more dramatic effects. Deletion of the C-terminal 36 residues of the SNARE domain (Syx1a (1–226)) weakens the interaction substantially: the  $K_d$  changes from 1 to 621 nM, and the binding enthalpy is reduced from  $-35$  to  $-8$  kcal/mol (Table I). Comparable results are obtained when the entire SNARE motif is deleted (Syx1a (1–179), Table I), indicating that Munc18a binds only weakly to the N-terminal region of syntaxin (i.e., the N-peptide + Habc). In agreement with a previous report (Wu *et al*, 1999), the mutation I233A, which is in the C-terminal section of the H3-domain of syntaxin 1a and directly contacts Munc18a, exhibits a strongly reduced affinity of 333 nM (Table I), corroborating the importance of this region for the strength of the Munc18a–syntaxin 1a interaction.

The syntaxin 1a N-peptide is required for Munc18 to bind to the assembled ternary SNARE complex (Dulubova *et al*, 2007; Shen *et al*, 2007), but it is less clear which other regions of the SNARE complex contribute to this interaction. ITC experiments confirmed that there is no detectable interaction between Munc18a and the SNARE complex formed with N-terminally truncated syntaxin 1a, Syx1a (25–262). In

contrast, the SNARE complex containing Syx1a (1–262) binds to Munc18a, albeit with relatively low affinity ( $K_d = 720$  nM, Table I). Importantly, both the affinity and binding enthalpy of the SNARE complex are identical within error to those of the isolated N-terminal region of syntaxin 1a, Syx1a (1–179). This suggests that the N-peptide and Habc domain of syntaxin 1a mediate the binding of Munc18a to the assembled SNARE complex, whereas there is no significant energetic contribution provided by the four-helix bundle region. This is consistent with data demonstrating that the Habc domain is flexibly linked to the H3 domain when the latter is part of the four-helix bundle SNARE complex (Margittai *et al*, 2003).

#### Role of the N-peptide in controlling SNARE complex assembly

To assess the functional effect of the syntaxin N-peptide, we made use of the SDS resistance of assembled neuronal SNARE complexes (Hayashi *et al*, 1994). When Syx1a (1–262) or Syx1a (25–262) were mixed with SNAP-25 and synaptobrevin, SDS-resistant complexes formed over time. When Munc18a and Syx1a (1–262) were pre-mixed, hardly any SDS-resistant complex was formed upon addition of SNAP-25 and synaptobrevin. In contrast, when Syx1a (25–262) was pre-mixed with Munc18a, a clear SDS-resistant SNARE complex band appeared (Figure 4A and B). Therefore, binding of the syntaxin 1a N-peptide to Munc18a is required to block SNARE complex formation. Earlier studies using syntaxin constructs starting at residue Arg4 also found that Munc18a blocked SNARE assembly (Pevsner *et al*, 1994; Yang *et al*, 2000); it is not clear what affinity tag residues preceded Arg4, but apparently they allow the N-peptide to bind (see also Supplementary data).

The effect of the N-peptide on SNARE complex formation was investigated more quantitatively using fluorescence-based assays in solution. When a fluorescently labelled cytosolic domain of synaptobrevin 2 was mixed with SNAP-25 and Syx1a (1–262) or Syx1a (25–262) in the absence of Munc18a, an increase in fluorescence anisotropy corresponding to the formation of a ternary SNARE complex was observed. As was seen in the SDS resistance assay, pre-mixing Munc18a with Syx1a (1–262) produced an almost complete block of ternary SNARE complex formation, whereas no inhibition was found when Munc18a and Syx1a

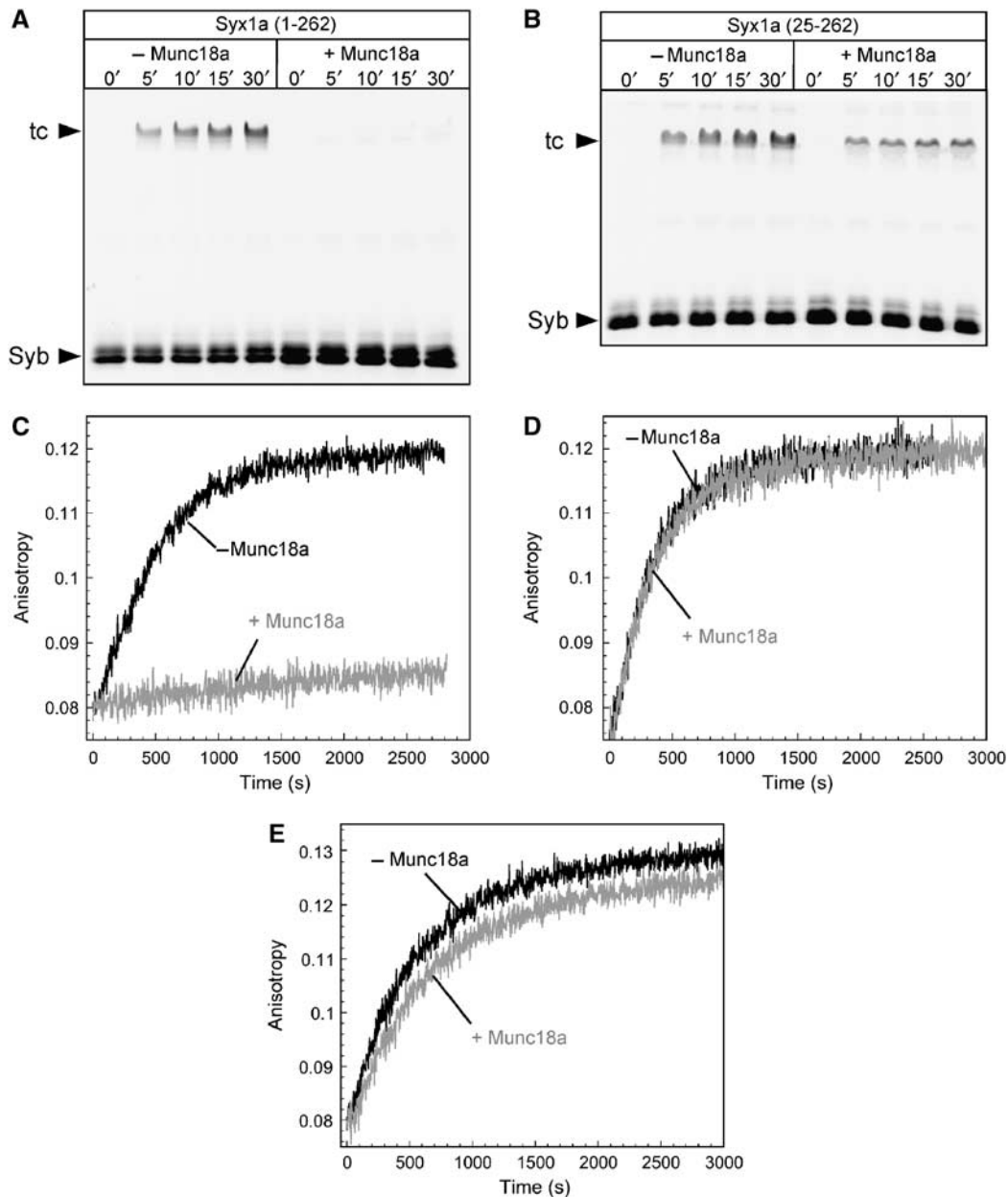


**Figure 4** Removal of the N-peptide of syntaxin allows for SNARE complex formation of Munc18-bound syntaxin. (A, B) Assembly of SNARE complexes in the absence or presence of Munc18a was monitored by the formation of SDS-resistant complexes containing synaptobrevin (Syb1–96) labelled with the fluorescent dye Alexa-488 at Cys79. For both syntaxin 1a variants, Syx1a (1–262) and Syx1a (25–262), SNARE complexes formed in the absence of Munc18a. In the presence of Munc18a, however, SNARE complex formation was abolished for Syx1a (1–262) (A), whereas a clear SDS-resistant band was visible for Syx1a (25–262) (B). Note that the SDS-resistant band in the presence of Munc18a appears to be weaker than that in the absence of Munc18a. This might be due to the fact Munc18a, which runs at the same molecular mass as the SDS-resistant SNARE complex, interfered with the intensity of the fluorescent band. (C–E) Ternary SNARE complex formation was followed by the increase in fluorescence anisotropy of 40 nM fluorescent Syb1–96 upon mixing with 500 nM syntaxin 1a and 750 nM SNAP-25. Munc18a (750 nM) inhibited SNARE complex formation for Syx1a (1–262) (C), but not for Syx1a (25–262) (D) and the ‘open’ syntaxin variant Syx<sup>LE</sup> (E). Note that for Syx1a (25–262) SNARE complex assembly occurred at about similar speed as in the absence of Munc18a.

(25–262) were pre-mixed (Figure 4C and D). Comparable results were obtained for the binary complex of syntaxin and SNAP-25 believed to be the intermediate in SNARE complex formation: binding of fluorescently labelled SNAP-25 to Syx1a (1–262), but not Syx1a (25–262), was inhibited by Munc18a (Supplementary Figure 3). The importance of the N-peptide in blocking SNARE assembly was also examined using point mutants of Syx1a (1–262) that do or do not significantly affect the affinity of the N-peptide (see above

and Table I). Syx1a (T5A) and Syx1a (T10A) blocked SNARE complex formation, whereas Syx1a (R4A) and Syx1a (L8A) allowed formation in the presence of Munc18a (Supplementary Figure 4), albeit with lower efficiency than in the absence of the N-peptide, that is, using Syx1a (25–262).

As Syx1a (25–262) binds with high affinity to Munc18a, it is surprising that this interaction does not prevent SNARE complex assembly (Figure 4B and D; Supplementary Figure 3). Therefore, we compared the kinetics of the

interaction of Munc18a to syntaxin 1a constructs containing or lacking the N-peptide. Binding of Munc18a to either syntaxin construct is approximately 10 000 times faster than binding of SNAP-25 to syntaxin (Supplementary Figure 1). The dissociation of the Munc18a–Syx1a (1–262) complex is very slow ( $t_{1/2} \approx 15$  min). In good agreement with a slightly reduced affinity for the Munc18a–Syx1a (25–262) interaction, the syntaxin 1a construct lacking the N-peptide dissociated about six times more rapidly from Munc18a ( $t_{1/2} \approx 2.5$  min, Supplementary Figure 1). The difference in rates for Munc18 versus SNAP-25 binding to syntaxin 1a is incompatible with a requirement for syntaxin to dissociate from Munc18a before it can bind to SNAP-25. Rather, the data strongly suggest that binding of SNAP-25 occurs when Munc18a is still bound to syntaxin 1a. Given the differences in the ability of syntaxin 1a constructs containing or lacking the N-peptide to participate in SNARE assembly in the presence of Munc18a, it is likely that the N-peptide influences the conformation of the Munc18a–syntaxin 1a complex such that in its absence syntaxin can bind to SNAP-25.

### **Munc18a binds tightly to, but does not block SNARE complex assembly of, the open syntaxin 1a variant**

The linker between the syntaxin Habc and H3 domains, residues 155–185, contains a short  $\alpha$  helix (residues 161–170) that forms intramolecular contacts with residues in Habc and H3 that are thought to stabilize the closed conformation of syntaxin (Misura *et al*, 2000). In addition, Glu166 lies near an electrostatically positive region of Munc18a domain 3a (Misura *et al*, 2000). The double mutant L165A/E166A (Syx1<sup>LE</sup>) was reported to abolish binding to Munc18a in pull-down assays (Dulubova *et al*, 1999), although the interaction is detectable in yeast two-hybrid assays (Dulubova *et al*, 2003). This mutation likely destabilizes the closed conformation by removing a critical hydrophobic contact with Habc and H3 (Misura *et al*, 2000). When analysed by ITC, Syx1<sup>LE</sup> binds to Munc18a with a  $K_d$  of 8 nM (Table I) and exhibits association and dissociation kinetics similar to those of Syx1a (25–262) (Supplementary Figure S1). Moreover, the LE mutant binds much more strongly than a mutant lacking the H3 SNARE domain (Syx1a (1–179)) and with the same enthalpy as full-length syntaxin ( $\Delta H = -35$  kcal/mol, Table I), implying that the H3 domain of the LE mutant does in fact interact with Munc18a. Indeed, we detected no binding of Munc18a to the isolated H3 domain of syntaxin 1a (Syx1a (180–262)), but addition of Syx1a (180–262) to the Munc18a–Syx1a (1–179) complex produced a ternary complex with increased stability relative to the binary interaction with Syx1a (1–179) (Table I), implying that in the presence of the rest of syntaxin H3 can interact with Munc18a even when the linker is severed.

The presence of Munc18a only slightly slowed the interaction of Syx1a<sup>LE</sup> with its partner SNAREs, despite the fact that this variant contains the N-peptide (Figure 4E; Supplementary Figure 5). As found for the Syx1a (1–262) and Syx1a (25–262) constructs, the kinetics of Syx1a<sup>LE</sup> binding to SNAP-25 (Supplementary Figure 1) are incompatible with its dissociation from Munc18a before binding to SNAP-25. Thus, although Syx1a<sup>LE</sup> is still tightly bound by Munc18a, its H3 domain is accessible to SNAP-25. The magnitude of the change in intrinsic fluorescence upon interaction with its SNARE partners was always slightly reduced for Syx1a<sup>LE</sup>

compared with wild-type syntaxin 1a (Supplementary Figure 1), suggesting a small conformational difference between the wild-type and mutant syntaxins. These observations support the notion that the contacts formed by the syntaxin linker helix both with the rest of syntaxin and with domain 3a of Munc18a are essential for the inhibition of SNARE assembly.

### **Vps45 also exhibits two modes of interaction with a cognate syntaxin**

Our findings on the Munc18a–syntaxin 1a interaction prompted us to re-inspect the binding mode of the SM protein Vps45 to syntaxin 16, which are believed to interact only through the N-peptide of syntaxin 16 (Dulubova *et al*, 2002). When measured by ITC, the isolated syntaxin 16 N-peptide, Syx16 (1–27), binds to Vps45 with a  $K_d$  of 27 nM and a binding enthalpy of  $-11.6$  kcal/mol (Figure 5). Similar binding affinity and enthalpy were seen when a larger fragment of syntaxin 16 that includes the Habc domain, Syx16 (1–183), was used (Table I). However, the entire cytosolic region of syntaxin 16, Syx16 (1–302), shows a markedly higher affinity ( $K_d \approx 1$  nM) and binding enthalpy ( $\Delta H = -23.8$  kcal/mol, Figure 5). In contrast to the situation in Syx1a–Munc18a, however, no binding of syntaxin 16 lacking the N-peptide, Syx16 (28–302), was detectable. Thus, it appears that both the N-peptide and the remaining portion of syntaxin 16 mediate high-affinity binding to Vps45, but with different energetic contributions relative to syntaxin 1a binding to Munc18a.

Interestingly, when we introduced a point mutation F10A in the N-peptide of the full syntaxin 16 cytosolic region (Syx16 (1–302)), which had previously described to largely abolish binding (Dulubova *et al*, 2002), we detected binding at reduced affinity ( $K_d \approx 117$  nM, Table I). However, when the same mutation was introduced into the isolated syntaxin 16 N-peptide, Syx16 (1–27, F10A), no binding was detectable. Thus, as in the Munc18a–syntaxin 1a complex, the N-peptide and the remaining portion of syntaxin 16 cooperate for high-affinity binding to Vps45. To test whether syntaxin 16 adopts a similar conformation as syntaxin 1a in the complex with the

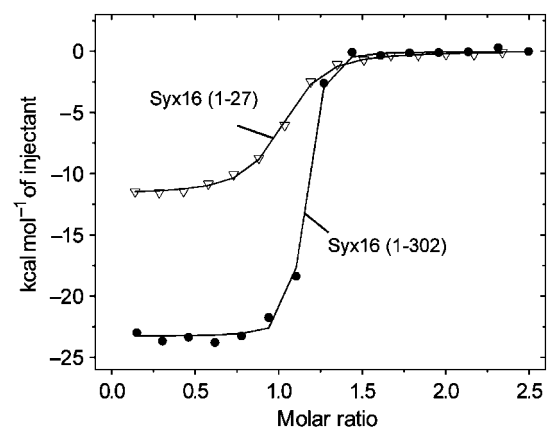


**Figure 5** The two binding sites Vps45 and syntaxin 16. Calorimetric titrations of syntaxin 16 (1–302 or 1–27) into Vps45. Shown are the integrated areas normalized to the amount of syntaxin 16 (kcal/mol) versus its molar ratio to Vps45. The solid lines represent the best fit to the data for a single-binding-site model using a nonlinear least squares fit.

SM protein, we used C-terminally shortened fragments of syntaxin 16 lacking part of the SNARE domain. Syx16 (1–279), which corresponds to Syx1a (1–240), bound with 1 nM affinity to Vps45. However, a shorter fragment, Syx16 (1–265), which corresponds to Syx1a (1–226), interacted with a reduced affinity of 12 nM. This indicates an interaction between the C-terminal portion of the syntaxin 16 SNARE domain and Vps45 equivalent to that of syntaxin 1a with the central cavity of Munc18a. The simplest interpretation of these data is that syntaxin 16 can form a closed conformation that binds to Vps45 similarly to the interaction of syntaxin 1a with Munc18a.

## Discussion

The interaction of SM proteins with the SNARE machinery is known to be essential for the fusion of transport vesicles with their target organelle. The two mechanistically distinct modes of interaction of SM proteins with their cognate syntaxins described so far have been thought to represent different functions of these proteins. Binding of an SM protein to the N-peptide of a syntaxin has been proposed to facilitate SNARE complex formation (Bracher and Weissenhorn, 2002; Dulubova *et al*, 2002; Peng and Gallwitz, 2002, 2004; Carpp *et al*, 2006; Latham *et al*, 2006), but no direct evidence or a well-defined mechanism for this role have been described. In contrast, binding to the closed conformation of syntaxin 1a by Munc18a prevents syntaxin from engaging its partner SNAREs (Pevsner *et al*, 1994; Dulubova *et al*, 1999; Misura *et al*, 2000; Yang *et al*, 2000). Recently, it was shown that Munc18a can also bind to an assembled SNARE complex, and this requires the syntaxin 1a N-peptide (Dulubova *et al*, 2007; Shen *et al*, 2007). It was therefore proposed that binding to the SNARE complex reflects a function common to all SM proteins, whereas binding to the closed conformation reflects a specific function of the neuronal syntaxin-SM pair. However, this notion does not reconcile the well-known inhibitory role of Munc18a on SNARE assembly (Pevsner *et al*, 1994; Dulubova *et al*, 1999; Misura *et al*, 2000; Yang *et al*, 2000) with its essential role in neurosecretion (for review, see Burgoyne and Morgan, 2007; Toonen and Verhage, 2007).

We have shown here that the high-affinity ( $K_d \approx 1$  nM) binary interaction of Munc18a and syntaxin 1a involves contacts with both the N-peptide and the closed conformation of syntaxin 1a, consistent with other recent reports (Khvotchev *et al*, 2007; Rickman *et al*, 2007). Remarkably, removal of the syntaxin N-peptide only slightly lowers the affinity, but completely relieves the inhibition exerted by Munc18a on the accessibility of the bound syntaxin for its SNARE partners. Thus, Munc18a-bound syntaxin is only able to form a SNARE complex when the N-peptide is released from Munc18a, contrary to the proposal that Munc18a stays bound to the N-peptide of syntaxin when the remainder of the molecule assembles into a SNARE complex (Khvotchev *et al*, 2007). If binding to the assembled SNARE complex is an essential function of Munc18a, then our finding that the N-peptide and Habc domains are required for this interaction implies that the N-peptide must rebind sometime after syntaxin interacts with SNAP-25.

Recently, the binary Munc18a–syntaxin 1a interaction was shown to be essential for vesicular docking, whereas an

interaction between Munc18a and syntaxin not requiring the closed syntaxin conformation appears to be essential for downstream priming reactions (Gulyas-Kovacs *et al*, 2007). However, the mechanistic roles of these two modes of interaction and the transformation between them remain unclear. A reasonable model is that when the syntaxin N-peptide is bound, Munc18a prevents inappropriate SNARE complex assembly. Interaction of the Munc18–syntaxin complex with upstream docking factors required for coordinating vesicle tethering with SNARE assembly or priming would control the binding status of the syntaxin N-peptide, insuring that productive *trans* pairing of SNAREs occurs at the correct location and time. This model implies that binding of Munc18a to the closed conformation and to the N-peptide of syntaxin 1a do not represent functionally distinct modes (Dulubova *et al*, 2007; Khvotchev *et al*, 2007; Shen *et al*, 2007), but are rather two aspects of the same function.

A plausible mechanism for the role of the syntaxin N-peptide is that binding of the N-peptide to the outer face of Munc18a stabilizes the interaction between the syntaxin H3 domain and the arch formed by Munc18a domains 1 and 3a. Comparison of the Munc18a–syntaxin 1a complex structure presented here with structures of unbound squid Munc18a reveals differences in the relative positions of domain 1 as well as differences in domain 3a (Bracher and Weissenhorn, 2001). In particular, the portion of domain 3a that lies near the syntaxin Habc-H3 linker, as well as other portions of syntaxin, is disordered in the absence of syntaxin. The N-peptide and H3-binding sites are linked by a chain of polar interactions that runs through the Munc18a domain 1–2 interface, so it appears that the two binding sites are coupled through this portion of Munc18a. The observation that the ‘open’ Syx1a<sup>LE</sup> mutant containing the N-peptide binds tightly to Munc18a, but allows SNARE complex formation, is consistent with such coupling. Removing the interactions of the Habc-H3 linker helix with syntaxin H3 and Munc18a domain 3a likely alters the conformation of the complex in a manner similar to that produced by removal of the N-peptide, thereby allowing SNAP-25 binding even when the N-peptide is bound to Munc18a. Structural studies aimed at understanding the allosteric regulation of H3 binding by the N-peptide are underway.

Our model also explains previously incoherent genetic and biochemical findings on Syx1a<sup>LE</sup>. First, in *Caenorhabditis elegans* Syx1a<sup>LE</sup> has been shown to rescue a syntaxin null mutant. Although Syx1a<sup>LE</sup> can bypass the requirement of Unc13 (Richmond *et al*, 2001; Hammarlund *et al*, 2007) and Rim (Koushika *et al*, 2001), factors that function in vesicle priming, it is unable to bypass Unc18 (Weimer *et al*, 2003), the *C. elegans* homologue of Munc18. The latter finding was unexpected as an already open form of syntaxin was anticipated not to require the action of Munc18. The cooperative binding mode described here suggests that Munc18a operates as a switch that first locks syntaxin 1a, thereby controlling its accessibility (N-peptide bound), while in the next step assists syntaxin 1a in forming a SNARE complex (N-peptide released). Hence, like wild-type syntaxin 1a, the open syntaxin variant must pass through the interaction with Munc18a, which serves as an essential template for binding to syntaxin. Second, the original experiments that reported no binding between Munc18a and Syx1a<sup>LE</sup> used brain homogenate as the source of Munc18a (Dulubova *et al*, 1999). The strong



Munc18a-Syx1a<sup>LE</sup> interaction may not have been observed in this case, because brain homogenate also contains the SNARE partners of syntaxin 1a, which could form the SNARE complex with Syx1<sup>LE</sup> in the presence of Munc18a. In fact, Syx1a<sup>LE</sup> mostly coprecipitated SNAP-25 and synaptobrevin, and the authors found an increased amount of complexin (Dulubova *et al*, 1999), which is a soluble protein that only binds to an assembled ternary SNARE complex (Pabst *et al*, 2002).

Our data support the idea that SNAP-25, possibly together with synaptobrevin, can directly bind to Munc18a-bound syntaxin 1a to form an intermediate in the SNARE complex assembly pathway. A similar notion has recently been suggested for Munc18a based on experiments using exocytosis-competent lawns of plasma membrane (Zilly *et al*, 2006). This putative assembly must be weak or transient, as we were unable to isolate it by size-exclusion chromatography. *In vivo*, however, a tripartite complex of Munc18a, syntaxin 1a, and SNAP-25 might be stabilized by additional factors. The configuration of this assembly, however, is probably different from that of Munc18a bound to the assembled neuronal SNARE complex (Dulubova *et al*, 2007; Shen *et al*, 2007).

The physiological role of the low-affinity ( $K_d \approx 0.7 \mu\text{M}$ ) Munc18a-SNARE complex interaction remains unclear. Although we have confirmed the interaction of Munc18a with the assembled SNARE complex (Dulubova *et al*, 2007; Shen *et al*, 2007), the data indicate that Munc18a binds to the N-peptide and Habc domain of syntaxin 1a in the SNARE complex, but not to the four-helix bundle formed by the interacting SNAREs. Although this explains why Munc18a can bind to syntaxin as part of the SNARE complex, it does not explain how this interaction is related to SNARE complex formation or membrane fusion. One study suggested that Munc18a participates in the establishment of the membrane fusion pore (Fisher *et al*, 2001), a step that is thought to occur after complete zipping of the SNARE complex, but this finding has been questioned (Gulyas-Kovacs *et al*, 2007). Most *in vivo* studies indicate a role for Munc18a in docking of the neurotransmitter-loaded vesicle and in priming of the secretory machinery. In these processes, Munc18 appears to operate in conjunction with syntaxin 1a, but not with the vesicular SNARE synaptobrevin (Toonen and Verhage, 2007), suggesting that the role of Munc18 is to control syntaxin and to assist its assembly with its SNARE partners, as discussed above. On the other hand, it has been shown that Munc18a stimulates SNARE-mediated liposome fusion (Shen *et al*, 2007), although the accelerating effect was far smaller than that observed in fusion experiments in which a stabilized t-SNARE acceptor site, in a ratio of 1:1, was used (Pobbati *et al*, 2006). It should also be noted that the accelerating effect of Munc18a was only observed when the SM protein was preincubated for several hours at 4°C with t-SNARE and v-SNARE liposomes. It thus cannot be excluded that Munc18a mostly affected the status of the t-SNARE, which in these experiments might have mostly resided in fusion-incompetent syntaxin-SNAP-25 complexes exhibiting a 2:1 stoichiometry.

We have shown here that high-affinity binding of another SM-syntaxin pair (Vps45-syntaxin 16), also requires two binding sites, the N-peptide and the remainder of the syntaxin molecule, the latter probably in a closed conformation. This suggests that an interaction involving two spatially distinct

binding sites may occur in other SM-syntaxin pairs. Indeed, point mutations in the SM protein Sly1 or in the N-peptide of Sed5 that interfere with N-peptide binding are still functional *in vivo* (Peng and Gallwitz, 2004), suggesting that additional regions of Sed5 are involved in the interaction. Comparable results have been obtained for the interaction of Vps45 and Tlg2 (Carpp *et al*, 2006). Likewise, syntaxin 4 appears to employ other regions than its N-peptide for the interaction with Munc18c (Latham *et al*, 2006; D'Andrea-Merrins *et al*, 2007), consistent with the notion of multiple binding sites. The data presented here indicate that the relative energetic contribution of each binding site is different for each SM-syntaxin pair. It is important to note that deletions of the N-peptide due to cloning artefacts or unexpected thrombin cleavage, or the addition of N-terminal residues from an affinity tag, can ablate the N-peptide interactions, which might explain some conflicting observations in the literature (Supplementary Figure 2). Further experiments will be needed to assess whether binding of the N-peptide also serves to control SNARE assembly in other SM-syntaxin pairs.

## Materials and methods

### Protein constructs

All proteins were derived from rat (*Rattus norvegicus*) and were cloned, if not indicated otherwise, into a pET28a vector that contains an N-terminal, thrombin-cleavable His<sub>6</sub>-tag. The basic bacterial expression constructs for SNARE proteins, such as cysteine-free SNAP-25A (1–206), the soluble portion of syntaxin 1a, Syx1a (1–262), the H3-domain of syntaxin 1a, Syx1a (180–262), and the soluble portion of synaptobrevin 2 (Syb1–96), have been described before. Likewise, the single-cysteine SNARE protein variants used for labelling with a fluorescent dye, for example SNAP-25 Cys130, Syb2 Cys79, and Syx1a (1–262) Cys 197, have been published (Fasshauer *et al*, 1999; Margittai *et al*, 2001; Fasshauer and Margittai, 2004). Full-length Munc18a, Vps45, and several truncated syntaxin 1a variants were constructed: Syx1a (1–240); Syx1a (1–226); Syx1a (1–179); Syx1a (25–206). In addition, syntaxin 1a constructs (aa 1–262) containing the point mutations I233A (Syx1a (I233A)), L165A and E166A (Syx1a<sup>LE</sup>), R4A (Syx1a (R4A)), T5A (Syx1a (T5A)), L8A (Syx1a (L8A)), T10A (Syx1a (T10A)), and S14A (Syx1a (S14A)) were generated. For Syx1a<sup>LE</sup> and Syx1a (25–206), cysteine variants at position 197 were constructed. Furthermore, the following syntaxin 16 constructs were used: Syx16 (1–302), Syx16 (1–279), Syx16 (1–265), Syx16 (1–183), Syx16 (28–302), and Syx16 containing the point mutation F10A, Syx16 (1–302, F10A). In addition, the following syntaxin 1a constructs with other affinity tags were used: Syx1a (1–267) in the pQE9 vector encoding a protein with an N-terminal, uncleavable His<sub>6</sub>-tag (Misura *et al*, 2000); Syx1a (1–265) in a modified pET11 vector (pHO4c) with a short, uncleavable C-terminal His<sub>6</sub>-tag (Fasshauer *et al*, 1999); Syx1a (1–267) in a modified pGEX-KG vector with a TEV-protease cleavable GST tag; Syx1a (1–266) in the pTwin1 vector with an intein-mediated self-cleaving chitin-binding domain affinity tag (an overview is given in Supplementary Figure 2).

### Protein purification

Recombinant proteins were purified by Ni<sup>2+</sup>-NTA or glutathione-affinity chromatography followed by ion-exchange chromatography essentially as described by Fasshauer *et al* (1999). SNARE complexes consisting of Syx1a (1–262 or 25–262), SNAP-25, and Syb2 (1–96) were assembled from purified components and purified by ion-exchange chromatography. His<sub>6</sub>-tags were generally removed using thrombin, but thrombin was omitted during the purification of syntaxin 1a constructs and SNARE complexes containing syntaxin 1a, as we found that thrombin also removes the first nine N-terminal residues of syntaxin 1a (see Supplementary Figure 3). Peptides comprising the N-peptide of syntaxin 1a, Syx1a (1–20), syntaxin 16, (Syx16 (1–27)), and with the point mutation F10A, Syx16 (1–27, F10A), were synthesized.

For analysis of the effects of non-native residues at the N terminus of syntaxin on the Munc18–syntaxin interaction, syntaxin 1–266 with no extra residues was purified using the pTwin1-syn1a (1–266) construct. Protein was purified from *Escherichia coli* by chitin-affinity chromatography, and the affinity tag was removed by addition of 40 mM DTT. The cleaved syntaxin was aggregated, and was therefore denatured in 8 M urea and refolded into 20 mM Tris pH 8, 500 mM NaCl. In addition, a syntaxin variant with the sequence GGIL at the N-terminus was purified using the pGEX-TEV syntaxin (1–267) construct. Here, protein was purified from *E. coli* by glutathione affinity column, and the GST tag was removed with TEV protease. In each case, the final purification step was anion-exchange chromatography using a HiTrapQ column (GE Healthcare).

#### Isothermal titration calorimetry

ITC was performed on a VP-ITC instrument (Microcal) at 25°C. Samples were dialysed against degassed PBS buffer (20 mM sodium phosphate, pH 7.4, 150 mM NaCl, 1 mM DTT) or Tris buffer (20 mM Tris pH 8.0, 150 mM NaCl, 1 mM DTT, 1 mM EDTA). Titrations were usually carried out by 20 µl, 15 µl, or 10 µl injections. The measured heat released on binding was integrated and analysed with Microcal Origin 7.0 using a single-site binding model, yielding the equilibrium association constant  $K_a$ , the enthalpy of binding  $\Delta H$ , and the stoichiometry  $n$ .

#### Fluorescence spectroscopy

All measurements were carried out in a Fluorolog 3 spectrometer in T-configuration equipped for polarization (Model FL322, Horiba Jobin Yvon). Single-cysteine variants were labelled with Texas Red C5 bromoacetamide, Oregon Green 488 iodoacetamide, or Alexa 488 C5 maleimide according to the manufacturer's instructions (Invitrogen). All experiments were performed at 25°C in 1-cm quartz cuvettes (Hellma) in PBS buffer. Measurements of fluorescence anisotropy, which reports the local flexibility of the labelled residue and which increases upon complex formation, were carried essentially as described (Fasshauer and Margittai, 2004; Pobbati *et al*, 2006). The G factor was calculated according to  $G = I_{HV}/I_{HH}$ , where  $I$  is the fluorescence intensity, and the first subscript letter indicates the direction of the exciting light and the second subscript letter the direction of the emitted light. The intensities of the vertically (V) and horizontally (H) polarized emission light after excitation by vertically polarized light were measured. The anisotropy ( $r$ ) was determined according to  $r = (I_{VV} - G I_{VH}) / (I_{VV} + 2 G I_{VH})$ . Intrinsic fluorescence measurements were performed at an excitation wavelength of 295 nm. Emission spectra were recorded in the range of 305–450 nm. All spectra were corrected for background fluorescence from buffer. The association of Munc18a and syntaxin 1a was measured using the Stopped-flow Device F-3009 (Horiba Jobin Yvon). The data were analysed using the Pro-KII software (Applied Photophysics).

#### Structure refinement

Prior to manual rebuilding of the structure of the Munc18a–syntaxin1a complex, the published coordinates (1DN1.pdb) were refined against the deposited structure factors by simulated annealing, coordinate minimization, and isotropic atomic temperature factor refinement in CNS version 1.2 (Brunger *et al*, 1998). In the resulting electron density maps, there was a large region of unmodelled electron density at the predicted binding site for the syntaxin N-peptide. Next, refinement was performed with phenix.-refine version 2007\_08\_18\_1856 (in the CCI Apps distribution). Each round of refinement with phenix used three macrocycles of coordinate minimization, TLS refinement using five TLS groups (corresponding to the subdomains of Munc18a and syntaxin), and isotropic atomic temperature factor refinement. The  $wxc\_scale$  parameter was set to 0.1. The improved electron density maps allowed for building of residues 2–9 of the syntaxin N-peptide using O (Jones and Kjeldgaard, 1997) and Coot (Emsley and Cowtan,

**Table II** Refinement statistics

Refinement	
Resolution (Å)	33.9–2.6
No. of reflections (work/free)	26 798/2332
$R_{work}/R_{free}$	0.203/0.263
<i>No. of atoms</i>	
Protein	6335
Water	69
<i>Average temperature factors</i>	
Protein	74.3
Water	51.2
<i>r.m.s.d.</i>	
Bond lengths (Å)	0.003
Bond angles (deg)	0.67
<i>Ramachandran analysis<sup>a</sup></i>	
Favored regions (%)	95.2
Additional allowed regions (%)	4.4
Outliers (%)	0.4

<sup>a</sup>From MOLPROBITY (Lovell *et al*, 2003).

2004). In addition, a number of minor errors in the deposited structure, including outliers in the Ramachandran plot and disallowed rotamers, were corrected. Thirty-five water molecules were also added. The re-refinement resulted in decreases in the  $R_{work}$  and  $R_{free}$  of 3.6 and 3.1%, respectively. As judged by Molprobity, the overall geometry of the re-refined structure is greatly improved (score of 98th percentile, versus 54th percentile for the starting model). Crystallographic figures were generated with Pymol (DeLano, 2002).

#### Electrophoretic procedures

SDS resistance of ternary SNARE complexes in polyacrylamide gels (Hayashi *et al*, 1994) was tested as described by Fasshauer *et al* (1999) with the modification that the complexes were visualized by the incorporation of synaptobrevin 2 labelled with the fluorescent dye Alexa-488 at cysteine 79.

#### Protein Data Bank accession code

Coordinates and structure factors of the newly refined crystal structure of the Munc18a–syntaxin 1a complex have been deposited in the Protein Data Bank under accession number 3C98.

#### Supplementary data

Supplementary data are available at *The EMBO Journal* Online (<http://www.embojournal.org>).

## Acknowledgements

We thank D Schütz, D Zwilling, D Bruns, and M Margittai for providing plasmids; F Lottspeich, U Pleßmann, and H Urlaub for support in protein analysis; W Berning-Koch for purifying proteins; T Siddiqui for help with the kinetic analysis; E Demircioglu for help with ITC measurements; and C Stegmann for valuable insights. We are indebted to A Stein, A Radakrishnan, K Wiederhold, U Winter, and R Jahn for critical reading of the manuscript. PB was supported by the Graduate Program 521 of the Deutsche Forschungsgemeinschaft. DAH and WIW were supported by grant MH58570 from the U.S. National Institutes of Health.

## References

Bracher A, Weissenhorn W (2001) Crystal structures of neuronal squid Sec1 implicate inter-domain hinge movement in the release of t-SNAREs. *J Mol Biol* **306**: 7–13

Bracher A, Weissenhorn W (2002) Structural basis for the Golgi membrane recruitment of Sly1p by Sed5p. *EMBO J* **21**: 6114–6124

- Brunger AT, Adams PD, Clore GM, DeLano WL, Gros P, Grosse-Kunstleve RW, Jiang JS, Kuszewski J, Nilges M, Pannu NS, Read RJ, Rice LM, Simonson T, Warren GL (1998) Crystallography & NMR system: a new software suite for macromolecular structure determination. *Acta Crystallogr D* **54**: 905–921
- Burgoyne RD, Morgan A (2007) Membrane trafficking: three steps to fusion. *Curr Biol* **17**: R255–R258
- Carpp LN, Ciuffo LF, Shanks SG, Boyd A, Bryant NJ (2006) The Sec1p/Munc18 protein Vps45p binds its cognate SNARE proteins via two distinct modes. *J Cell Biol* **173**: 927–936
- D'Andrea-Merrins M, Chang L, Lam AD, Ernst SA, Stuenkel EL (2007) Munc18c interaction with syntaxin 4 monomers and SNARE complex intermediates in GLUT4 vesicle trafficking. *J Biol Chem* **282**: 16553–16566
- DeLano WL (2002) *The PyMOL Molecular Graphics System*. Palo Alto, CA, USA: DeLano Scientific
- Dulubova I, Khvotchev M, Liu S, Huryeva I, Sudhof TC, Rizo J (2007) Munc18-1 binds directly to the neuronal SNARE complex. *Proc Natl Acad Sci USA* **104**: 2697–2702
- Dulubova I, Sugita S, Hill S, Hosaka M, Fernandez I, Südhof TC, Rizo J (1999) A conformational switch in syntaxin during exocytosis: role of munc18. *EMBO J* **18**: 4372–4382
- Dulubova I, Yamaguchi T, Arac D, Li H, Huryeva I, Min SW, Rizo J, Südhof TC (2003) Convergence and divergence in the mechanism of SNARE binding by Sec1/Munc18-like proteins. *Proc Natl Acad Sci USA* **100**: 32–37
- Dulubova I, Yamaguchi T, Gao Y, Min SW, Huryeva I, Südhof TC, Rizo J (2002) How Tlg2p/syntaxin 16 'snares' Vps45. *EMBO J* **21**: 3620–3631
- Emsley P, Cowtan K (2004) Coot: model-building tools for molecular graphics. *Acta Crystallogr D* **60**: 2126–2132
- Fasshauer D, Antonin W, Margittai M, Pabst S, Jahn R (1999) Mixed and non-cognate SNARE complexes. Characterization of assembly and biophysical properties. *J Biol Chem* **274**: 15440–15446
- Fasshauer D, Margittai M (2004) A transient N-terminal interaction of SNAP-25 and syntaxin nucleates SNARE assembly. *J Biol Chem* **279**: 7613–7621
- Fernandez I, Ubach J, Dulubova I, Zhang X, Südhof TC, Rizo J (1998) Three-dimensional structure of an evolutionarily conserved N-terminal domain of syntaxin 1A. *Cell* **94**: 841–849
- Fisher RJ, Pevsner J, Burgoyne RD (2001) Control of fusion pore dynamics during exocytosis by Munc18. *Science* **291**: 875–878
- Gallwitz D, Jahn R (2003) The riddle of the Sec1/Munc-18 proteins—new twists added to their interactions with SNAREs. *Trends Biochem Sci* **28**: 113–116
- Gulyas-Kovacs A, de Wit H, Milosevic I, Kochubey O, Toonen R, Klingauf J, Verhage M, Sorensen JB (2007) Munc18-1: sequential interactions with the fusion machinery stimulate vesicle docking and priming. *J Neurosci* **27**: 8676–8686
- Hammarlund M, Palfreyman MT, Watanabe S, Olsen S, Jorgensen EM (2007) Open syntaxin docks synaptic vesicles. *PLoS Biol* **5**: e198
- Hayashi T, McMahon H, Yamasaki S, Binz T, Hata Y, Südhof TC, Niemann H (1994) Synaptic vesicle membrane fusion complex: action of clostridial neurotoxins on assembly. *EMBO J* **13**: 5051–5061
- Hong W (2005) SNAREs and traffic. *Biochim Biophys Acta* **1744**: 493–517
- Hu SH, Latham CF, Gee CL, James DE, Martin JL (2007) Structure of the Munc18c/Syntaxin4 N-peptide complex defines universal features of the N-peptide binding mode of Sec1/Munc18 proteins. *Proc Natl Acad Sci USA* **104**: 8773–8778
- Jahn R, Scheller RH (2006) SNAREs—engines for membrane fusion. *Nat Rev Mol Cell Biol* **7**: 631–643
- Jones TA, Kjeldgaard M (1997) Electron density map interpretation. *Methods Enzymol* **277**: 173–208
- Khvotchev M, Dulubova I, Sun J, Dai H, Rizo J, Südhof TC (2007) Dual modes of Munc18-1/SNARE interactions are coupled by functionally critical binding to syntaxin-1 N terminus. *J Neurosci* **27**: 12147–12155
- Koushika SP, Richmond JE, Hadwiger G, Weimer RM, Jorgensen EM, Nonet ML (2001) A post-docking role for active zone protein Rim. *Nat Neurosci* **4**: 997–1005
- Latham CF, Lopez JA, Hu SH, Gee CL, Westbury E, Blair DH, Armishaw CJ, Alewood PF, Bryant NJ, James DE, Martin JL (2006) Molecular dissection of the Munc18c/syntaxin4 interaction: implications for regulation of membrane trafficking. *Traffic* **7**: 1408–1419
- Lovell SC, Davis IW, Arendall III WB, de Bakker PI, Word JM, Prisant MG, Richardson JS, Richardson DC (2003) Structure validation by Calpha geometry: phi, psi and Cbeta deviation. *Proteins* **50**: 437–450
- Margittai M, Fasshauer D, Jahn R, Langen R (2003) The Habc domain and the SNARE core complex are connected by a highly flexible linker. *Biochemistry* **42**: 4009–4014
- Margittai M, Fasshauer D, Pabst S, Jahn R, Langen R (2001) Homomeric and heterooligomeric snare complexes studied by site-directed spin labeling. *J Biol Chem* **276**: 13169–13177
- Misura KM, Scheller RH, Weis WI (2000) Three-dimensional structure of the neuronal-Sec1-syntaxin 1a complex. *Nature* **404**: 355–362
- Pabst S, Margittai M, Vainius D, Langen R, Jahn R, Fasshauer D (2002) Rapid and selective binding to the synaptic SNARE complex suggests a modulatory role of complexins in neuro-exocytosis. *J Biol Chem* **277**: 7838–7848
- Peng R, Gallwitz D (2002) Sly1 protein bound to Golgi syntaxin Sed5p allows assembly and contributes to specificity of SNARE fusion complexes. *J Cell Biol* **157**: 645–655
- Peng R, Gallwitz D (2004) Multiple SNARE interactions of an SM protein: Sed5p/Sly1p binding is dispensable for transport. *EMBO J* **23**: 3939–3949
- Pevsner J, Hsu SC, Braun JE, Calakos N, Ting AE, Bennett MK, Scheller RH (1994) Specificity and regulation of a synaptic vesicle docking complex. *Neuron* **13**: 353–361
- Pobbati A, Stein A, Fasshauer D (2006) N- to C-terminal SNARE complex assembly promotes rapid membrane fusion. *Science* **313**: 673–676
- Richmond JE, Weimer RM, Jorgensen EM (2001) An open form of syntaxin bypasses the requirement for UNC-13 in vesicle priming. *Nature* **412**: 338–341
- Rickman C, Medine CN, Bergmann A, Duncan RR (2007) Functionally and spatially distinct modes of munc18-syntaxin 1 interaction. *J Biol Chem* **282**: 12097–12103
- Rizo J, Südhof TC (2002) Snares and Munc18 in synaptic vesicle fusion. *Nat Rev Neurosci* **3**: 641–653
- Scott BL, Van Komen JS, Irshad H, Liu S, Wilson KA, McNew JA (2004) Sec1p directly stimulates SNARE-mediated membrane fusion *in vitro*. *J Cell Biol* **167**: 75–85
- Shen J, Tarest DC, Paumet F, Rothman JE, Melia TJ (2007) Selective activation of Cognate SNAREpins by Sec1/Munc18 proteins. *Cell* **128**: 183–195
- Togneri J, Cheng YS, Munson M, Hughson FM, Carr C (2006) Specific SNARE complex binding mode of the Sec1/Munc-18 protein, Sec1p. *Proc Natl Acad Sci USA* **103**: 17730–17735
- Toonen RF, Verhage M (2003) Vesicle trafficking: pleasure and pain from SM genes. *Trends Cell Biol* **13**: 177–186
- Toonen RF, Verhage M (2007) Munc18-1 in secretion: lonely Munc joins SNARE team and takes control. *Trends Neurosci* **30**: 564–572
- Weber T, Zemelman BV, McNew JA, Westermann B, Gmachl M, Parlati F, Sollner TH, Rothman JE (1998) SNAREpins: minimal machinery for membrane fusion. *Cell* **92**: 759–772
- Weimer RM, Richmond JE (2005) Synaptic vesicle docking: a putative role for the Munc18/Sec1 protein family. *Curr Top Dev Biol* **65**: 83–113
- Weimer RM, Richmond JE, Davis WS, Hadwiger G, Nonet ML, Jorgensen EM (2003) Defects in synaptic vesicle docking in unc-18 mutants. *Nat Neurosci* **6**: 1023–1030
- Wu MN, Fergestad T, Lloyd TE, He Y, Broadie K, Bellen HJ (1999) Syntaxin 1A interacts with multiple exocytic proteins to regulate neurotransmitter release *in vivo*. *Neuron* **23**: 593–605
- Yang B, Steegmaier M, Gonzalez Jr LC, Scheller RH (2000) nSec1 binds a closed conformation of syntaxin1A. *J Cell Biol* **148**: 247–252
- Zilly FE, Sorensen JB, Jahn R, Lang T (2006) Munc18-bound syntaxin readily forms SNARE complexes with synaptobrevin in native plasma membranes. *PLoS Biol* **4**: e330